

Topological optimization and minimal compliance in linear elasticity

Cornel Marius Murea¹, Dan Tiba²

¹ Département de Mathématiques, IRIMAS,

Université de Haute Alsace, France,

cornel.murea@uha.fr

² Institute of Mathematics (Romanian Academy) and
Academy of Romanian Scientists, Bucharest, Romania,

dan.tiba@imar.ro

Abstract

We investigate a fixed domain approach in shape optimization, using a regularization of the Heaviside function both in the cost functional and in the state system. We consider the compliance minimization problem in linear elasticity, a well known application in this area of research. The optimal design problem is approached by an optimal control problem defined in a prescribed domain including all the admissible unknown domains. This approximating optimization problem has good differentiability properties and a gradient algorithm can be applied. Moreover, the paper also includes several numerical experiments that demonstrate the descent of the obtained cost values and show the topological and the boundary variations of the computed domains. The proposed approximation technique is new and can be applied to state systems given by various boundary value problems.

Keywords: topological optimization; minimal compliance

1 Minimal compliance in linear elasticity

Let $\Omega \subset \mathbb{R}^2$ be a connected, bounded, Lipschitz domain with boundary $\partial\Omega = \bar{\Gamma}_D \cup \bar{\Gamma}_N \cup \bar{\Gamma}$, where Γ_D , Γ_N and Γ are relatively open subsets, mutually disjoint, such that $meas(\Gamma_D) > 0$, $meas(\Gamma_N) > 0$, $meas(\Gamma) > 0$.

The notation $\mathbf{v} \cdot \mathbf{w}$ means the scalar product of two vectors $\mathbf{v}, \mathbf{w} \in \mathbb{R}^2$ and $A : B =$

$\sum_{i,j=1}^2 a_{ij}b_{ij}$ if $A = (a_{ij})_{1 \leq i,j \leq 2}$, $B = (b_{ij})_{1 \leq i,j \leq 2}$. We will use

$$\nabla \cdot \mathbf{v} = \frac{\partial v_1}{\partial x_1} + \frac{\partial v_2}{\partial x_2}, \quad \nabla \cdot A = \begin{pmatrix} \frac{\partial a_{11}}{\partial x_1} + \frac{\partial a_{12}}{\partial x_2} \\ \frac{\partial a_{21}}{\partial x_1} + \frac{\partial a_{22}}{\partial x_2} \end{pmatrix}$$

to denote the divergence operator of a vector valued function $\mathbf{v} \in \mathbb{R}^2$ or $A = (a_{ij})_{1 \leq i,j \leq 2} \in \mathbb{R}^{2 \times 2}$.

We denote by $\mathbf{y} : \bar{\Omega} \rightarrow \mathbb{R}^2$ the displacement of the linear elastic body $\Omega \subset \mathbb{R}^2$. The stress tensor in linear elasticity is given by

$$\sigma(\mathbf{y}) = \lambda^S (\nabla \cdot \mathbf{y}) \mathbf{I} + 2\mu^S \mathbf{e}(\mathbf{y})$$

where $\lambda^S, \mu^S > 0$ are the Lamé coefficients, independent of the space variable, \mathbf{I} is the unity matrix and $\mathbf{e}(\mathbf{y}) = \frac{1}{2} (\nabla \mathbf{y} + (\nabla \mathbf{y})^T)$.

For given volume load $\mathbf{f} : \Omega \rightarrow \mathbb{R}^2$ and surface load $\mathbf{h} : \Gamma_N \rightarrow \mathbb{R}^2$, we consider the linear elasticity equations: find $\mathbf{y} : \bar{\Omega} \rightarrow \mathbb{R}^2$ such that

$$-\nabla \cdot \sigma(\mathbf{y}) = \mathbf{f}, \text{ in } \Omega \quad (1.1)$$

$$\mathbf{y} = 0, \text{ on } \Gamma_D \quad (1.2)$$

$$\sigma(\mathbf{y}) \mathbf{n} = \mathbf{h}, \text{ on } \Gamma_N \quad (1.3)$$

$$\sigma(\mathbf{y}) \mathbf{n} = 0, \text{ on } \Gamma \quad (1.4)$$

where \mathbf{n} is the unit outer normal vector along the boundary.

The weak formulation is: find $\mathbf{y} \in V$ such that

$$\int_{\Omega} \sigma(\mathbf{y}) : \nabla \mathbf{v} \, d\mathbf{x} = \int_{\Omega} \mathbf{f} \cdot \mathbf{v} \, d\mathbf{x} + \int_{\Gamma_N} \mathbf{h} \cdot \mathbf{v} \, ds, \quad \forall \mathbf{v} \in V \quad (1.5)$$

where $\mathbf{f} \in (L^2(\Omega))^2$, $\mathbf{h} \in (L^2(\Gamma_N))^2$,

$$V = \{\mathbf{v} \in (H^1(\Omega))^2; \mathbf{v} = 0 \text{ on } \Gamma_D\}.$$

It is well known that this problem has a unique solution in V , see [8].

Using that $\sigma(\mathbf{y})$ is symmetric and the identity $A : B = A^T : B^T$, we obtain that the left-hand side from (1.5) with $\mathbf{v} = \mathbf{y}$ satisfies:

$$\begin{aligned} \int_{\Omega} \sigma(\mathbf{y}) : \nabla \mathbf{y} \, d\mathbf{x} &= \int_{\Omega} \frac{1}{2} \sigma(\mathbf{y}) : \nabla \mathbf{y} + \frac{1}{2} \sigma(\mathbf{y}) : \nabla \mathbf{y} \, d\mathbf{x} \\ &= \int_{\Omega} \frac{1}{2} \sigma(\mathbf{y}) : \nabla \mathbf{y} + \frac{1}{2} (\sigma(\mathbf{y}))^T : (\nabla \mathbf{y})^T \, d\mathbf{x} \\ &= \int_{\Omega} \frac{1}{2} \sigma(\mathbf{y}) : \nabla \mathbf{y} + \frac{1}{2} \sigma(\mathbf{y}) : (\nabla \mathbf{y})^T \, d\mathbf{x} \\ &= \int_{\Omega} \sigma(\mathbf{y}) : \mathbf{e}(\mathbf{y}) \, d\mathbf{x} = \int_{\Omega} \lambda^S (\nabla \cdot \mathbf{y}) \mathbf{I} : \mathbf{e}(\mathbf{y}) + 2\mu^S \mathbf{e}(\mathbf{y}) : \mathbf{e}(\mathbf{y}) \, d\mathbf{x} \\ &= \int_{\Omega} \lambda^S (\nabla \cdot \mathbf{y})^2 + 2\mu^S \mathbf{e}(\mathbf{y}) : \mathbf{e}(\mathbf{y}) \, d\mathbf{x}. \end{aligned} \quad (1.6)$$

A classical problem in structural design, see [5], [6], [1], is to find a domain Ω that minimizes the compliance (the work done by the load, expressed by the right-hand side in (1.5) with $\mathbf{v} = \mathbf{y}$) subject to $\Gamma_N \subset \partial\Omega$, $\Gamma_D \subset \partial\Omega$ and the volume of Ω is prescribed, see Figure 1. We suppose that Γ_N and Γ_D are fixed. On Γ_D the elastic body Ω is also fixed due to (1.2), while Γ_N is fixed in the sense that this part of the boundary is specified in advance for the family of all admissible domains Ω and may deform under the action of the traction \mathbf{h} and the volume load \mathbf{f} in (1.3).

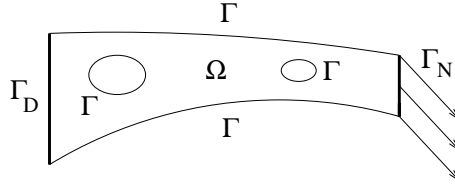


Figure 1: The geometrical configuration.

Here, we examine the minimization of the compliance as well as of the volume of Ω . In practice, we penalize the volume of Ω , and the function to minimize is

$$\int_{\Omega} \mathbf{f} \cdot \mathbf{y} \, d\mathbf{x} + \int_{\Gamma_N} \mathbf{h} \cdot \mathbf{y} \, ds + \ell \int_{\Omega} 1 \, d\mathbf{x} \quad (1.7)$$

where $\ell > 0$ is a penalization coefficient. The fixed domain method that we introduce here combines boundary variations with topology optimization (the domain Ω is not necessarily simply connected and the number of holes may change during the iterations). This is characterized by Γ , the part of $\partial\Omega$ that is not fixed. It is a new approach and another important property is that it may be applied to many boundary value problems as governing systems. For other fixed domain approaches, we quote [14], [15], [19], [20] and the survey [16] with its references. For multi-layered composite materials, one can consult [9].

2 The shape optimization problem in fixed domain and its gradient

We consider a simply connected, bounded, Lipschitz domain $D \subset \mathbb{R}^2$, including the unknown domain Ω , with $\partial D = \overline{\Sigma}_D \cup \overline{\Gamma}_N \cup \overline{\Sigma}$, where Σ_D , Γ_N and Σ are relatively open subsets, mutually disjoint, such that $\Gamma_D \subset \Sigma_D$, see Figure 2.

Let $X(D)$ denote a cone of $\mathcal{C}(\overline{D})$. Following [15], [16], with any $g \in X(D)$, that we call a parametrization, we associate the open set

$$\Omega_g = \text{int} \{ \mathbf{x} \in D; g(\mathbf{x}) \geq 0 \}.$$

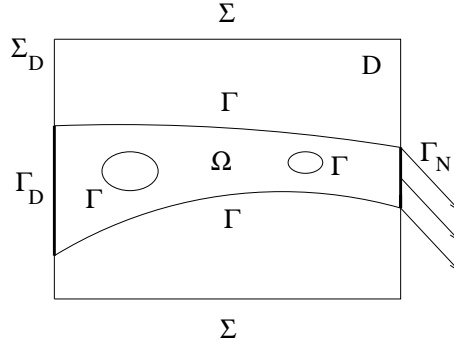


Figure 2: The fixed domain D including the unknown domain.

We define the family of admissible domains as the connected components of all Ω_g , $g \in X(D)$ satisfying $\Gamma_N \subset \partial\Omega_g$, $\Gamma_D \subset \partial\Omega_g$. This family is very rich and some examples are commented in Remark 2.1 below.

We use the following regularization of the Heaviside function

$$H^\epsilon(r) = \begin{cases} 1 - \frac{1}{2}e^{-\frac{r}{\epsilon}}, & r \geq 0, \\ \frac{1}{2}e^{\frac{r}{\epsilon}}, & r < 0, \end{cases} \quad (2.8)$$

where $\epsilon > 0$ is a parameter. We have that $H^\epsilon(g)$ is a regularization of the characteristic function of $\overline{\Omega}_g$. This procedure has already been introduced in [14]. Another approximation that we shall also use is $H_\epsilon(r) = 1$, $r \geq 0$ and $H_\epsilon(r) = \epsilon$, $r < 0$. The advantage of (2.8) is its differentiability.

For given $\mathbf{f} \in (L^2(D))^2$, $\mathbf{h} \in (L^2(\Gamma_N))^2$ and $\ell > 0$, we introduce the control problem (with control g) that approximates the shape optimization problem

$$\inf_{g \in X(D)} \left\{ J(g) = \int_D H^\epsilon(g) \mathbf{f} \cdot \mathbf{y}^\epsilon(g) \, d\mathbf{x} + \int_{\Gamma_N} \mathbf{h} \cdot \mathbf{y}^\epsilon(g) \, ds + \ell \int_D H^\epsilon(g) \, d\mathbf{x} \right\} \quad (2.9)$$

where $\mathbf{y}^\epsilon(g) \in W$ is the solution of

$$\int_D H^\epsilon(g) \sigma(\mathbf{y}^\epsilon(g)) : \nabla \mathbf{v} \, d\mathbf{x} = \int_D H^\epsilon(g) \mathbf{f} \cdot \mathbf{v} \, d\mathbf{x} + \int_{\Gamma_N} \mathbf{h} \cdot \mathbf{v} \, ds, \quad (2.10)$$

for all $\mathbf{v} \in W$, where

$$W = \{\mathbf{v} \in (H^1(D))^2; \mathbf{v} = 0 \text{ on } \Gamma_D\}.$$

We point out that $H^\epsilon(g) > 0$ in D and $H^\epsilon(g) \geq 1/2$ in $\overline{\Omega}_g$ due to (2.8). Moreover, $H^\epsilon(g)$ is an approximation of the characteristic function of $\overline{\Omega}_g$ and due to this, there is an approximation relation between the solutions of (2.10) and (1.5), that we examine in the sequel.

Regularization methods have a long history in fixed domain methods for problems involving unknown domains. For instance, already [13] used a penalization/regularization method in free boundary problems. A survey on this subject is the paper [16] and in [19], [17] such approaches are extended to the optimization of plates with holes and other problems. In general, Dirichlet boundary conditions are taken into account, while the approximation defined in (2.9), (2.10) can be used for other boundary conditions as well.

Remark 2.1 *An admissible domain Ω_g for $g \in \mathcal{C}(\overline{D})$ has to satisfy $\Gamma_N \subset \partial\Omega_g$, $\Gamma_D \subset \partial\Omega_g$, that can be obtained by imposing simple equality constraints on g (see below). Moreover, we also assume Ω_g to be connected, and this constraint has to be added to the definition of $X(D)$. However in the regularized problem, this is not necessary since we work in D . Other constraints on the geometry Ω_g may be included in the definition below, if necessary. For instance $E \subset \Omega_g$, where E is some given domain (add below the inequality $g > 0$ in E), etc.*

We set

$$X(D) = \{g \in \mathcal{C}(\overline{D}); g(\mathbf{x}) = 0, \mathbf{x} \in \Gamma_N \cup \Gamma_D\}$$

which is a subspace in $\mathcal{C}(\overline{D})$. If $g \in \mathcal{C}^1(D)$ and is noncritical on its null level set, then the condition from the beginning of this remark is satisfied. In general, $X(D)$ is a cone.

Proposition 2.1 *The problem (2.10) has a unique solution $\mathbf{y}^\epsilon(g) \in W$ and*

$$\|\mathbf{y}^\epsilon(g)\|_{1,D} \leq \frac{C}{c(\epsilon)} \left(\|\mathbf{f}\|_{0,D} + \|\mathbf{h}\|_{0,\Gamma_N} \right) \quad (2.11)$$

where $C > 0$ is independent of ϵ and $c(\epsilon) > 0$ is indicated below.

Proof. We set

$$a(\mathbf{y}, \mathbf{v}) = \int_D H^\epsilon(g) \sigma(\mathbf{y}) : \nabla \mathbf{v} \, d\mathbf{x}$$

and we get from (1.6):

$$\begin{aligned} a(\mathbf{v}, \mathbf{v}) &= \int_D H^\epsilon(g) \sigma(\mathbf{v}) : \nabla \mathbf{v} \, d\mathbf{x} \\ &= \int_D H^\epsilon(g) (\lambda^S (\nabla \cdot \mathbf{v})^2 + 2\mu^S \mathbf{e}(\mathbf{v}) : \mathbf{e}(\mathbf{v})) \, d\mathbf{x} \\ &\geq c(\epsilon) \int_D (\lambda^S (\nabla \cdot \mathbf{v})^2 + 2\mu^S \mathbf{e}(\mathbf{v}) : \mathbf{e}(\mathbf{v})) \, d\mathbf{x} \\ &\geq c(\epsilon) \int_D 2\mu^S \mathbf{e}(\mathbf{v}) : \mathbf{e}(\mathbf{v}) \, d\mathbf{x}. \end{aligned}$$

We have used that $H^\epsilon(g) \geq c(\epsilon) > 0$ in D , due to (2.8). In fact $c(\epsilon)$ also depends on g , that is fixed here (and uniformly bounded). From the Korn's inequality, see [8], we

obtain that a is W -elliptic, i.e. $a(\mathbf{v}, \mathbf{v}) \geq \frac{c(\epsilon)}{C} \|\mathbf{v}\|_{1,D}^2$, where $C > 0$ is independent on g , ϵ . From the Lax-Milgram theorem, we get that the problem has a unique solution and

$$\|\mathbf{y}^\epsilon(g)\|_{1,D} \leq \frac{C}{c(\epsilon)} \left(\|H^\epsilon(g)\mathbf{f}\|_{0,D} + \|\mathbf{h}\|_{0,\Gamma_N} \right) \leq \frac{C}{c(\epsilon)} \left(\|\mathbf{f}\|_{0,D} + \|\mathbf{h}\|_{0,\Gamma_N} \right).$$

since $0 < H^\epsilon(g) \leq 1$. \square

We indicate now some basic approximation results.

Proposition 2.2 *When $\epsilon \rightarrow 0$, on a subsequence, we have $\mathbf{y}^\epsilon|_{\Omega_g} \rightarrow \mathbf{y}$ weakly in $H^1(\Omega_g)$. Moreover, $\mathbf{y} \in V$ and satisfies (1.1) - (1.4) in the distributional sense. This statement remains valid for the corresponding approximating solutions when H^ϵ is replaced by H_ϵ in (2.10).*

Proof. Let $\mathbf{f}_1 \in L^2(D)$ be the extension by 0 of $\mathbf{f} \in L^2(\Omega_g)$. We use the approximating formulation (2.10) with \mathbf{f} replaced by \mathbf{f}_1 and $\mathbf{v} = \mathbf{y}_\epsilon \in W$:

$$\int_D H^\epsilon(g) \sigma(\mathbf{y}^\epsilon) : \nabla \mathbf{y}^\epsilon \, d\mathbf{x} = \int_D H^\epsilon(g) \mathbf{f}_1 \cdot \mathbf{y}^\epsilon \, d\mathbf{x} + \int_{\Gamma_N} \mathbf{h} \cdot \mathbf{y}^\epsilon \, ds. \quad (2.12)$$

By (1.6) and (2.12), we get

$$\begin{aligned} & \int_D H^\epsilon(g) [\lambda^S (\nabla \cdot \mathbf{y}^\epsilon)^2 + 2\mu^S \mathbf{e}(\mathbf{y}^\epsilon) : \mathbf{e}(\mathbf{y}^\epsilon)] \, d\mathbf{x} \\ &= \int_D H^\epsilon(g) \mathbf{f}_1 \cdot \mathbf{y}^\epsilon \, d\mathbf{x} + \int_{\Gamma_N} \mathbf{h} \cdot \mathbf{y}^\epsilon \, ds. \end{aligned} \quad (2.13)$$

In the left-hand side of (2.13), all the terms are positive, due to (2.8), and we infer the inequality

$$\mu^S \int_{\Omega_g} \mathbf{e}(\mathbf{y}^\epsilon) : \mathbf{e}(\mathbf{y}^\epsilon) \, d\mathbf{x} \leq \int_{\Omega_g} \mathbf{f} \cdot \mathbf{y}^\epsilon \, d\mathbf{x} + \int_{\Gamma_N} \mathbf{h} \cdot \mathbf{y}^\epsilon \, ds, \quad (2.14)$$

where we use that $1 \geq H^\epsilon(g) \geq 1/2$ in Ω_g and the definition of \mathbf{f}_1 . One can apply the Korn's inequality in (2.14) and establish that $\mathbf{y}^\epsilon|_{\Omega_g}$ is bounded in $H^1(\Omega_g)$. On a subsequence, $\mathbf{y}^\epsilon|_{\Omega_g} \rightarrow \mathbf{y}$ weakly in $H^1(\Omega_g)$. Moreover, $H^\epsilon(g) \rightarrow H(g)$ in $L^p(D)$, for any $p \geq 1$.

For any test function $\mathbf{v} \in \mathcal{D}(\Omega_g) \subset W$, we pass to the limit in (2.10) and obtain

$$\int_{\Omega_g} \sigma(\mathbf{y}) : \nabla \mathbf{v} \, d\mathbf{x} = \int_{\Omega_g} \mathbf{f} \cdot \mathbf{v} \, d\mathbf{x} + \int_{\Gamma_N} \mathbf{h} \cdot \mathbf{v} \, ds, \quad \forall \mathbf{v} \in \mathcal{D}(\Omega_g)$$

and the proof of the first part is finished.

For the last statement of Proposition 2.2, we denote by \mathbf{y}_ϵ the corresponding solution and we assume that $\mathbf{f} \in L^2(D)$ is given (we don't use the above extension by 0). We use the definition of H_ϵ and decompose (2.10) as follows

$$\begin{aligned} & \epsilon \int_D \sigma(\mathbf{y}_\epsilon) : \nabla \mathbf{v} \, d\mathbf{x} + (1 - \epsilon) \int_{\Omega_g} \sigma(\mathbf{y}_\epsilon) : \nabla \mathbf{v} \, d\mathbf{x} \\ &= \epsilon \int_D \mathbf{f} \cdot \mathbf{v} \, d\mathbf{x} + (1 - \epsilon) \int_{\Omega_g} \mathbf{f} \cdot \mathbf{v} \, d\mathbf{x} + \int_{\Gamma_N} \mathbf{h} \cdot \mathbf{v} \, ds, \quad \forall \mathbf{v} \in W. \end{aligned} \quad (2.15)$$

Putting $\mathbf{v} = \mathbf{y}_\epsilon$ in (2.15), it is easy to see, by using the identity (1.6) and Korn's inequality in D , that the difference between the two terms with coefficient ϵ from (2.15) is bounded from below by some constant. The other terms are handled as above, using Korn's inequality in Ω_g and we get that \mathbf{y}_ϵ is bounded in $H^1(\Omega_g)$ if $\epsilon \leq 1/2$. The passage to the limit is as above. \square

Remark 2.2 *Concerning shape optimization problems and their approximation, it is advantageous to use H^ϵ due to the differentiability properties that will be discussed below. When g is the unknown control and may change, the procedure to extend \mathbf{f} by 0 outside the $\text{supp}(\mathbf{f})$ (from the first part of the proof) involves the hypothesis that $g \geq 0$ in $\text{supp}(\mathbf{f})$, for any admissible g . The numerical examples from the last section confirm that our method allows topological and boundary variations and ensures a good descent of the cost.*

Proposition 2.3 *For any g, w in $X(D)$, the mapping $g \rightarrow \mathbf{y}^\epsilon(g) \in W$ is Gâteaux differentiable at g and the directional derivative in the direction w , denoted by $\mathbf{z} \in W$, is the unique solution of the problem*

$$\begin{aligned} & \int_D H^\epsilon(g) \sigma(\mathbf{z}) : \nabla \mathbf{v} \, d\mathbf{x} = \\ & - \int_D (H^\epsilon)'(g) w \sigma(\mathbf{y}^\epsilon(g)) : \nabla \mathbf{v} \, d\mathbf{x} + \int_D (H^\epsilon)'(g) w \mathbf{f} \cdot \mathbf{v} \, d\mathbf{x}, \quad \forall \mathbf{v} \in W. \end{aligned} \quad (2.16)$$

Proof. Let g, w be fixed in $X(D)$ and $\lambda \neq 0$, small. We notice first that $X(D)$ is stable to small perturbations, i.e. $g + \lambda w \in X(D)$ if $|\lambda|$ small.

We write the equation (2.10) for $g + \lambda w$ and the corresponding solution $\mathbf{y}^\epsilon(g + \lambda w)$

$$\begin{aligned} & \int_D H^\epsilon(g + \lambda w) \sigma(\mathbf{y}^\epsilon(g + \lambda w)) : \nabla \mathbf{v} \, d\mathbf{x} \\ &= \int_D H^\epsilon(g + \lambda w) \mathbf{f} \cdot \mathbf{v} \, d\mathbf{x} + \int_{\Gamma_N} \mathbf{h} \cdot \mathbf{v} \, ds, \quad \forall \mathbf{v} \in W. \end{aligned}$$

Subtracting (2.10) from the above equation, we obtain

$$\begin{aligned} & \int_D H^\epsilon(g + \lambda w) \sigma(\mathbf{y}^\epsilon(g + \lambda w)) : \nabla \mathbf{v} \, d\mathbf{x} - \int_D H^\epsilon(g) \sigma(\mathbf{y}^\epsilon(g)) : \nabla \mathbf{v} \, d\mathbf{x} \\ &= \int_D H^\epsilon(g + \lambda w) \mathbf{f} \cdot \mathbf{v} \, d\mathbf{x} - \int_D H^\epsilon(g) \mathbf{f} \cdot \mathbf{v} \, d\mathbf{x}, \quad \forall \mathbf{v} \in W. \end{aligned}$$

Now, subtracting and adding the term $\int_D H^\epsilon(g + \lambda w) \sigma(\mathbf{y}^\epsilon(g)) : \nabla \mathbf{v} \, d\mathbf{x}$ in the first line, dividing by λ , setting $\mathbf{z}_\lambda^\epsilon = \frac{\mathbf{y}^\epsilon(g + \lambda w) - \mathbf{y}^\epsilon(g)}{\lambda}$, we get

$$\begin{aligned} & \int_D H^\epsilon(g + \lambda w) \sigma(\mathbf{z}_\lambda^\epsilon) : \nabla \mathbf{v} \, d\mathbf{x} = - \int_D \frac{H^\epsilon(g + \lambda w) - H^\epsilon(g)}{\lambda} \sigma(\mathbf{y}^\epsilon(g)) : \nabla \mathbf{v} \, d\mathbf{x} \\ & + \int_D \frac{H^\epsilon(g + \lambda w) - H^\epsilon(g)}{\lambda} \mathbf{f} \cdot \mathbf{v} \, d\mathbf{x}, \quad \forall \mathbf{v} \in W. \end{aligned} \quad (2.17)$$

Since $H^\epsilon \in \mathcal{C}^2(\mathbb{R})$, for each $y_0, h \in \mathbb{R}$, there exists $\xi \in \mathbb{R}$ such that

$$H^\epsilon(y_0 + h) = H^\epsilon(y_0) + h(H^\epsilon)'(y_0) + \frac{h^2}{2}(H^\epsilon)''(\xi),$$

then, for each $\mathbf{x} \in \overline{D}$, there exists $\xi_x \in \mathbb{R}$ such that

$$\frac{H^\epsilon(g(\mathbf{x}) + \lambda w(\mathbf{x})) - H^\epsilon(g(\mathbf{x}))}{\lambda} = w(\mathbf{x})(H^\epsilon)'(g(\mathbf{x})) + \frac{\lambda}{2} w^2(\mathbf{x})(H^\epsilon)''(\xi_x).$$

But, by construction $(H^\epsilon)''$ is bounded in \mathbb{R} (ϵ is fixed) and $w \in \mathcal{C}(\overline{D})$ is bounded in the compact \overline{D} . It follows that, for all $\delta \in (0, 1)$, there exists $\lambda_1(\delta) > 0$ such that

$$\left\| \frac{H^\epsilon(g + \lambda w) - H^\epsilon(g)}{\lambda} - (H^\epsilon)'(g) w \right\|_{\mathcal{C}(\overline{D})} \leq \delta, \quad \forall |\lambda| < \lambda_1(\delta), \quad \lambda \neq 0. \quad (2.18)$$

Then $\frac{H^\epsilon(g + \lambda w) - H^\epsilon(g)}{\lambda}$ converges to $(H^\epsilon)'(g) w$ in $\mathcal{C}(\overline{D})$, for $\lambda \rightarrow 0$. We get that

$$\left\| \frac{H^\epsilon(g + \lambda w) - H^\epsilon(g)}{\lambda} \right\|_{\mathcal{C}(\overline{D})} \leq M, \quad \forall |\lambda| < \lambda_1(\delta), \quad \lambda \neq 0 \quad (2.19)$$

where $M = M(\epsilon)$ is independent of λ , but depends on ϵ .

As in Proposition 2.1, we can obtain the estimate for $\mathbf{z}_\lambda^\epsilon \in W$

$$\begin{aligned} \|\mathbf{z}_\lambda^\epsilon\|_{1,D} &\leq \frac{C M}{c(\epsilon)} \left(\|\sigma(\mathbf{y}^\epsilon(g))\|_{0,D} + \|\mathbf{f}\|_{0,D} \right) \\ &\leq \frac{C M}{c(\epsilon)} \left(C_1 \|\mathbf{y}^\epsilon(g)\|_{1,D} + \|\mathbf{f}\|_{0,D} \right) \end{aligned} \quad (2.20)$$

where $C_1 > 0$ is independent of λ, ϵ such that $\|\sigma(\mathbf{v})\|_{0,D} \leq C_1 \|\mathbf{v}\|_{1,D}$, for all $\mathbf{v} \in W$.

Let $\tilde{\mathbf{z}} \in W$ such that, on a subsequence $\mathbf{z}_\lambda^\epsilon$ converges weakly to $\tilde{\mathbf{z}}$ in W and strongly in $(L^2(D))^2$. For passing to the limit on a subsequence in (2.17), we use Lemma 6.1 from [11]: if $a, a_n \in L^\infty(D)$, $\|a_n\|_{0,\infty,D} \leq M$, $a_n \rightarrow a$ almost everywhere in D , $b_n \rightarrow b$ weakly in $L^2(D)$ and $h \in L^2(D)$, then

$$\lim_{n \rightarrow \infty} \int_D a_n b_n h \, dx = \int_D a b h \, dx.$$

We can apply this Lemma for $a_n = H^\epsilon(g + \lambda_n w)$, $b_n = \sigma(\mathbf{z}_{\lambda_n}^\epsilon)$ and $h = \nabla \mathbf{v}$. By passing to the limit on a subsequence in (2.17) we get that $\tilde{\mathbf{z}}$ is solution of (2.16). But, as in Proposition 2.1, we can show that the problem (2.16) has a unique solution, then $\tilde{\mathbf{z}} = \mathbf{z}$ and $\mathbf{z}_\lambda^\epsilon$ converges to \mathbf{z} for $\lambda \rightarrow 0$ without taking subsequence, weakly in W and strongly in $(L^2(D))^2$.

Now, we will prove that $\mathbf{z}_\lambda^\epsilon$ converges to \mathbf{z} strongly in W . Subtracting (2.16) from (2.17), we get

$$\begin{aligned} & \int_D H^\epsilon(g + \lambda w) \sigma(\mathbf{z}_\lambda^\epsilon) : \nabla \mathbf{v} \, d\mathbf{x} - \int_D H^\epsilon(g) \sigma(\mathbf{z}) : \nabla \mathbf{v} \, d\mathbf{x} \\ = & - \int_D \left(\frac{H^\epsilon(g + \lambda w) - H^\epsilon(g)}{\lambda} - (H^\epsilon)'(g)w \right) \sigma(\mathbf{y}^\epsilon(g)) : \nabla \mathbf{v} \, d\mathbf{x} \\ & + \int_D \left(\frac{H^\epsilon(g + \lambda w) - H^\epsilon(g)}{\lambda} - (H^\epsilon)'(g)w \right) \mathbf{f} \cdot \mathbf{v} \, d\mathbf{x}. \end{aligned} \quad (2.21)$$

Subtracting and adding the term $\int_D H^\epsilon(g) \sigma(\mathbf{z}_\lambda^\epsilon(g)) : \nabla \mathbf{v} \, d\mathbf{x}$ in the first line, transferring some terms at the right-hand side, we get

$$\begin{aligned} & - \int_D H^\epsilon(g) \sigma(\mathbf{z}) : \nabla \mathbf{v} \, d\mathbf{x} + \int_D H^\epsilon(g) \sigma(\mathbf{z}_\lambda^\epsilon) : \nabla \mathbf{v} \, d\mathbf{x} \\ = & - \int_D \left(\frac{H^\epsilon(g + \lambda w) - H^\epsilon(g)}{\lambda} - (H^\epsilon)'(g)w \right) \sigma(\mathbf{y}^\epsilon(g)) : \nabla \mathbf{v} \, d\mathbf{x} \\ & + \int_D \left(\frac{H^\epsilon(g + \lambda w) - H^\epsilon(g)}{\lambda} - (H^\epsilon)'(g)w \right) \mathbf{f} \cdot \mathbf{v} \, d\mathbf{x} \\ & - \int_D (H^\epsilon(g + \lambda w) - H^\epsilon(g)) \sigma(\mathbf{z}_\lambda^\epsilon) : \nabla \mathbf{v} \, d\mathbf{x}. \end{aligned} \quad (2.22)$$

At the left-hand side of (2.22), we have $a(\mathbf{z}_\lambda^\epsilon - \mathbf{z}, \mathbf{v})$. Taking into account (2.18) and (2.19), the right-hand side of (2.22) can be estimated by

$$\begin{aligned} & \delta \left(\|\sigma(\mathbf{z}_\lambda^\epsilon)\|_{0,D} + \|\mathbf{f}\|_{0,D} \right) \|\mathbf{v}\|_{0,D} + \lambda M \|\sigma(\mathbf{z}_\lambda^\epsilon)\|_{0,D} \|\mathbf{v}\|_{0,D} \\ \leq & \delta \left((1 + M)C_1 \|\mathbf{z}_\lambda^\epsilon\|_{1,D} + \|\mathbf{f}\|_{0,D} \right) \|\mathbf{v}\|_{0,D} \end{aligned}$$

for all $|\lambda| < \min(\delta, \lambda_1(\delta))$, $\lambda \neq 0$, where $C_1 > 0$ such that $\|\sigma(\mathbf{v})\|_{0,D} \leq C_1 \|\mathbf{v}\|_{1,D}$, for all $\mathbf{v} \in W$.

Finally, from (2.20), (2.11) and for $\mathbf{v} = \mathbf{z}_\lambda^\epsilon - \mathbf{z}$, we obtain

$$\frac{c(\epsilon)}{C} \|\mathbf{z}_\lambda^\epsilon - \mathbf{z}\|_{1,D}^2 \leq a(\mathbf{z}_\lambda^\epsilon - \mathbf{z}, \mathbf{z}_\lambda^\epsilon - \mathbf{z}) \leq \delta C_3(\epsilon) \left(\|\mathbf{f}\|_{0,D} + \|\mathbf{h}\|_{0,\Gamma_N} \right) \|\mathbf{z}_\lambda^\epsilon - \mathbf{z}\|_{1,D}$$

and after simplification, we get that $\|\mathbf{z}_\lambda^\epsilon - \mathbf{z}\|_{1,D} \leq \delta \frac{C C_3(\epsilon)}{c(\epsilon)} \left(\|\mathbf{f}\|_{0,D} + \|\mathbf{h}\|_{0,\Gamma_N} \right)$ for all $\delta \in (0, 1)$. Then $\mathbf{z}_\lambda^\epsilon$ converges to \mathbf{z} strongly in W , when λ tends to 0, but ϵ is fixed.

The linearity and the continuous dependence of its solution on the right-hand side (on w) in equation (2.16) shows the Gâteaux differentiability and ends the proof. \square

Proposition 2.4 *The directional derivative of the objective function (2.9) has the form*

$$\begin{aligned} J'(g)w &= \int_D H^\epsilon(g) \mathbf{f} \cdot \mathbf{z} \, d\mathbf{x} + \int_D (H^\epsilon)'(g) w \mathbf{f} \cdot \mathbf{y}^\epsilon(g) \, d\mathbf{x} \\ &+ \int_{\Gamma_N} \mathbf{h} \cdot \mathbf{z} \, ds + \ell \int_D (H^\epsilon)'(g) w \, d\mathbf{x} \end{aligned} \quad (2.23)$$

for any g, w in $X(D)$.

Proof. Let g, w be fixed in $X(D)$ and $\lambda \neq 0$. We get

$$\begin{aligned} \frac{J(g + \lambda w) - J(g)}{\lambda} &= \frac{1}{\lambda} \int_D (H^\epsilon(g + \lambda w) \mathbf{f} \cdot \mathbf{y}^\epsilon(g + \lambda w) - H^\epsilon(g) \mathbf{f} \cdot \mathbf{y}^\epsilon(g)) \, d\mathbf{x} \\ &+ \int_{\Gamma_N} \mathbf{h} \cdot \frac{\mathbf{y}^\epsilon(g + \lambda w) - \mathbf{y}^\epsilon(g)}{\lambda} \, ds \\ &+ \ell \int_D \frac{H^\epsilon(g + \lambda w) - H^\epsilon(g)}{\lambda} \, d\mathbf{x} \end{aligned} \quad (2.24)$$

From the Proposition 2.3, $\mathbf{z}_\lambda^\epsilon = \frac{\mathbf{y}^\epsilon(g + \lambda w) - \mathbf{y}^\epsilon(g)}{\lambda}$ converges strongly to \mathbf{z} in W . By the trace theorem on Γ_N , we get $\mathbf{z}_\lambda^\epsilon|_{\Gamma_N}$ converges strongly to $\mathbf{z}|_{\Gamma_N}$ in $(L^2(\Gamma_N))^2$. Consequently, the term of the second line in (2.24) converges to $\int_{\Gamma_N} \mathbf{h} \cdot \mathbf{z} \, ds$.

From (2.18), $\frac{H^\epsilon(g + \lambda w) - H^\epsilon(g)}{\lambda}$ converges uniformly to $(H^\epsilon)'(g) w$ in $\mathcal{C}(\overline{D})$, for $\lambda \rightarrow 0$, consequently, the term of the third line in (2.24) converges to $\ell \int_D (H^\epsilon)'(g) w \, d\mathbf{x}$.

It remains to study the right-hand side of the first line of (2.24). Subtracting and

adding $\int_D H^\epsilon(g + \lambda w) \mathbf{y}^\epsilon(g) : \nabla \mathbf{v} \, d\mathbf{x}$, dividing by λ , we get

$$\begin{aligned} & \frac{1}{\lambda} \int_D (H^\epsilon(g + \lambda w) \mathbf{y}^\epsilon(g + \lambda w) - H^\epsilon(g + \lambda w) \mathbf{y}^\epsilon(g)) \cdot \mathbf{f} \, d\mathbf{x} \\ & + \frac{1}{\lambda} \int_D (H^\epsilon(g + \lambda w) \mathbf{y}^\epsilon(g) - H^\epsilon(g) \mathbf{y}^\epsilon(g)) \cdot \mathbf{f} \, d\mathbf{x} \\ = & \int_D H^\epsilon(g + \lambda w) \frac{\mathbf{y}^\epsilon(g + \lambda w) - \mathbf{y}^\epsilon(g)}{\lambda} \cdot \mathbf{f} \, d\mathbf{x} \\ & + \int_D \frac{H^\epsilon(g + \lambda w) - H^\epsilon(g)}{\lambda} \mathbf{y}^\epsilon(g) \cdot \mathbf{f} \, d\mathbf{x} \end{aligned}$$

We have that $H^\epsilon(g + \lambda w)$ converges uniformly to $H^\epsilon(g)$ in $\mathcal{C}(\overline{D})$. Using once again that $\mathbf{z}_\lambda^\epsilon$ converges strongly to \mathbf{z} in W and $\frac{H^\epsilon(g + \lambda w) - H^\epsilon(g)}{\lambda}$ converges uniformly to $(H^\epsilon)'(g)w$ in $\mathcal{C}(\overline{D})$, we get that the right-hand side of the first line of (2.24) converges to $\int_D H^\epsilon(g) \mathbf{z} \cdot \mathbf{f} \, d\mathbf{x} + \int_D (H^\epsilon)'(g)w \mathbf{y}^\epsilon(g) \cdot \mathbf{f} \, d\mathbf{x}$. \square

We can give an expression of the directional derivative of $J(g)$ without using \mathbf{z} .

Proposition 2.5 *For any g, w in $X(D)$, we have*

$$J'(g)w = \int_D (H^\epsilon)'(g)w [2\mathbf{f} \cdot \mathbf{y}^\epsilon(g) + \ell - \sigma(\mathbf{y}^\epsilon(g)) : \nabla \mathbf{y}^\epsilon(g)] \, d\mathbf{x}. \quad (2.25)$$

Proof. From (2.10), we put $\mathbf{v} = \mathbf{z} \in W$ and using (see (1.6))

$$\sigma(\mathbf{y}^\epsilon(g)) : \nabla \mathbf{z} = \lambda^S (\nabla \cdot \mathbf{y}^\epsilon(g)) (\nabla \cdot \mathbf{z}) + 2\mu^S \mathbf{e}(\mathbf{y}^\epsilon(g)) \mathbf{e}(\mathbf{z}) = \sigma(\mathbf{z}) : \nabla \mathbf{y}^\epsilon(g)$$

we get

$$\int_D H^\epsilon(g) \sigma(\mathbf{z}) : \nabla \mathbf{y}^\epsilon(g) \, d\mathbf{x} = \int_D H^\epsilon(g) \mathbf{f} \cdot \mathbf{z} \, d\mathbf{x} + \int_{\Gamma_N} \mathbf{h} \cdot \mathbf{z} \, ds. \quad (2.26)$$

Putting $\mathbf{v} = \mathbf{y}^\epsilon(g)$ in (2.16), it follows

$$\begin{aligned} & \int_D H^\epsilon(g) \sigma(\mathbf{z}) : \nabla \mathbf{y}^\epsilon(g) \, d\mathbf{x} \\ = & - \int_D (H^\epsilon)'(g)w \sigma(\mathbf{y}^\epsilon(g)) : \nabla \mathbf{y}^\epsilon(g) \, d\mathbf{x} + \int_D (H^\epsilon)'(g)w \mathbf{f} \cdot \mathbf{y}^\epsilon(g) \, d\mathbf{x}. \end{aligned} \quad (2.27)$$

From (2.26) and (2.27), we obtain

$$\begin{aligned} & \int_D H^\epsilon(g) \mathbf{f} \cdot \mathbf{z} \, d\mathbf{x} + \int_{\Gamma_N} \mathbf{h} \cdot \mathbf{z} \, ds \\ = & - \int_D (H^\epsilon)'(g)w \sigma(\mathbf{y}^\epsilon(g)) : \nabla \mathbf{y}^\epsilon(g) \, d\mathbf{x} + \int_D (H^\epsilon)'(g)w \mathbf{f} \cdot \mathbf{y}^\epsilon(g) \, d\mathbf{x} \end{aligned}$$

and taking into account (2.23), we get the conclusion. \square

Remark 2.3 *By the above result, one can obtain the form of the gradient of the cost and avoid the use of an adjoint system.*

In the following, we present some descent directions for the objective function. We set

$$d = 2\mathbf{f} \cdot \mathbf{y}^\epsilon(g) + \ell - \sigma(\mathbf{y}^\epsilon(g)) : \nabla \mathbf{y}^\epsilon(g)$$

and since

$$\sigma(\mathbf{y}^\epsilon(g)) : \nabla \mathbf{y}^\epsilon(g) = \sigma(\mathbf{y}^\epsilon(g)) : \mathbf{e}(\mathbf{y}^\epsilon(g)) = \lambda^S (\nabla \cdot \mathbf{y}^\epsilon(g))^2 + 2\mu^S \mathbf{e}(\mathbf{y}^\epsilon(g)) : \mathbf{e}(\mathbf{y}^\epsilon(g))$$

then

$$d = 2\mathbf{f} \cdot \mathbf{y}^\epsilon(g) + \ell - (\lambda^S (\nabla \cdot \mathbf{y}^\epsilon(g))^2 + 2\mu^S \mathbf{e}(\mathbf{y}^\epsilon(g)) : \mathbf{e}(\mathbf{y}^\epsilon(g))). \quad (2.28)$$

We have only $d \in L^1(D)$, in general.

We use, as in [19] the function $R : \mathbb{R} \rightarrow \mathbb{R}$ defined by

$$R(r) = \begin{cases} c(-1 + e^r), & r < 0, \\ c(1 - e^{-r}), & r \geq 0 \end{cases} \quad (2.29)$$

where $c > 0$. The function R is strictly increasing, $R(\mathbb{R}) =]-c, c[$, $R(-r) = -R(r)$ and $r R(r) \geq 0$ for all $r \in \mathbb{R}$.

Proposition 2.6 *For d given by (2.28), the following are descent directions for the objective function $J(g)$:*

$$i) \quad w_d = -H^\epsilon(g)d \quad (2.30)$$

$$ii) \quad w_d = -H^\epsilon(g)R(d) \quad (2.31)$$

$$iii) \quad w_d = -\tilde{d} \quad (2.32)$$

under the assumption that $w_d \in X(D)$. At *iii*), $\tilde{d} \in H^1(D)$ is the solution of

$$\int_D \gamma(\nabla \tilde{d} \cdot \nabla v) + \tilde{d} v \, d\mathbf{x} = \int_D (H^\epsilon)'(g) d v \, d\mathbf{x}, \quad \forall v \in H^1(D) \quad (2.33)$$

and $\gamma > 0$ is a parameter.

Proof. It is a consequence of Proposition 2.5. In the case *i*), we have

$$J'(g)w_d = \int_D (H^\epsilon)'(g)w_d d \, d\mathbf{x} = - \int_D (H^\epsilon)'(g)H^\epsilon(g)d^2 \, d\mathbf{x} < 0$$

since $0 < (H^\epsilon)'(r)$, $0 < H^\epsilon(r)$, for all $r \in \mathbb{R}$.

In the case ii), we have

$$J'(g)w_d = - \int_D (H^\epsilon)'(g)H^\epsilon(g) d R(d) d\mathbf{x} < 0$$

since $r R(r) > 0$ for all $r \in \mathbb{R}^*$. In the case iii), we have

$$J'(g)w_d = - \int_D (H^\epsilon)'(g)d\tilde{d}d\mathbf{x} = - \int_D \gamma(\nabla\tilde{d} \cdot \nabla\tilde{d}) + \tilde{d}\tilde{d}d\mathbf{x} < 0$$

since $\gamma > 0$. \square

Remark 2.4 *More generally, $w_d = -\alpha d$ and $w_d = -\alpha R(d)$, where $\alpha \in L^\infty(D)$ and $\alpha \geq 0$, $\alpha \neq 0$, are descent directions, too. For example, in the case i), we have $J'(g)w_d = - \int_D (H^\epsilon)'(g)d^2\alpha d\mathbf{x} < 0$, since $0 < (H^\epsilon)'(r)$ for all $r \in \mathbb{R}^*$, $d^2 \geq 0$, $\alpha \geq 0$. The case iii) is inspired by [7].*

3 Numerical examples

We have employed the software FreeFem++, [12]. The dimensions and the starting domains are from the web site of the team directed by G. Allaire [4], the files `levelset-cantilever.edp` and `pont.homog.struct.edp`.

Our approach decreases the cost and ensures both boundary and/or topology variations, including the creation of new holes.

Algorithm

Step 1 Let g_0 be the initial guess. Fix a bound N for the number of iterations and put $n := 0$.

Step 2 Let w_n be a descent direction of J in g_n , given by (2.30), (2.31), or (2.32).

Step 3 Compute the directional derivative $J'(g_n)w_n$ according to Proposition 2.5.

If $J'(g_n)w_n = 0$, then **Stop**.

Step 4 Find

$$\lambda_n \in \arg \min_{\lambda \in \mathbb{R}} J(g_n + \lambda w_n)$$

obtained via some line search and put $g_{n+1} = g_n + \lambda_n w_n$. Practically, we look for $\lambda = \rho^i$, $\rho \in (0, 1)$ and $i = 0, 1, \dots$. The maximal number of iterations for the line search is fixed to 10. Alternatively, we can use backtracking line search method, see [10] or other method.

Step 5 If $n + 1 = N$ then **Stop**

Step 6 If $|J(g_n) - J(g_{n+1})| < tol$ then **Stop**,

else update $n := n + 1$ and go to **Step 2**.

The final domains given by the above algorithm are not necessary globally optimal. In the following, optimal domain means final computed domain in the descent procedure.

In the previous sections, we have supposed that Γ_D and Γ_N are given. For the numerical tests, we assume that only $\Gamma_N \subset \partial D$ is given, but Γ_D is unknown. The space W for the weak formulation (2.10) is

$$W = \{\mathbf{v} \in (H^1(D))^2; \mathbf{v} = 0 \text{ on } \Sigma_D\}.$$

Generally, Σ_D is not a subset of $\partial\Omega_g$ and the Dirichlet boundary condition (1.2) is imposed in fact only on $\partial\Omega_g \cap \Sigma_D$. We set $\Gamma_D = \partial\Omega_g \cap \Sigma_D$. In terms of the control g , this can be ensured by imposing in the definition of $X(D)$ that $g(\mathbf{x}) < 0$, $\mathbf{x} \in \partial D \setminus [\Sigma_D \cup \Gamma_N]$ too (compare Remark 2.1).

If $\Omega_g \subset\subset D$, then $\mathbf{x} \in \partial\Omega_g$ yields $g(\mathbf{x}) = 0$. Otherwise, when $meas(\partial\Omega_g \cap \partial D) > 0$, it is possible $\mathbf{x} \in (\partial\Omega_g \cap \partial D)$ and $g(\mathbf{x}) > 0$.

The initial parametrization here satisfies $g_0(\mathbf{x}) > 0$, $\mathbf{x} \in \Gamma_N$ and $\Gamma_N \subset \partial\Omega_{g_0}$. Also, we have $meas(\partial\Omega_{g_0} \cap \Sigma_D) > 0$. For particular initial parametrizations used here, we have observed that $g_n(\mathbf{x}) > 0$, $\mathbf{x} \in \Gamma_N$ and $meas(\partial\Omega_{g_n} \cap \Sigma_D) > 0$ for all the iterations n until convergence. For different initial parametrization, this property may not hold systematically and should be imposed as a constraint on g .

Example 1. Cantilever

We have $D =]0, 2[\times] - 0.5, 0.5[$, $\Sigma_D = \{0\} \times] - 0.5, 0.5[$, $\Gamma_N = \{2\} \times] - 0.1, 0.1[$, see Figure 3, left. We work with Lamé coefficients $\lambda^S = 1$, $\mu^S = 8$ and $\rho = 0.6$. The volume load is $\mathbf{f} = (0, 0)$, the surface load on Γ_N is $\mathbf{h} = (0, -5)$ and the parameter in the objective function associated to the volume of the structure is $\ell = 0.5$.

We use for D a mesh of 45638 triangles and 23120 vertices. For the approximation of g and $H^\epsilon(g)$ we use piecewise linear finite element, globally continuous and for \mathbf{y} we use the finite element \mathbb{P}_2 , piecewise polynomial of degree two, see [18]. We set $\epsilon = 10^{-2}$ the penalization parameter and $tol = 10^{-6}$, $N = 50$ for the stopping tests.

The initial domain is obtained for $g_0(x_1, x_2) = 0.1 - \sin(4\pi x_1) \sin(3\pi(x_2 - 0.5))$ and the initial value of the objective function is $J(g_0) = 3.49524$. This starting domain is also used by [4]. It has many initial holes and the algorithm “closes” some of them, but also produces new holes as may be seen in Figure 4 and 5.

The history of the objective functions for descent directions *i*) and *ii*) given by (2.30) and (2.31) is presented in Figure 3 right, the optimal value is 2.24849 in the case *i*) after 50 iterations (**Step 5**) and 2.55336 in the case *ii*) after 38 iterations (**Step 6**). The stopping test **Step 3** is obtained for $n = 3$ for the descent direction *iii*) given by (2.32), (2.33) with $\gamma = 0.001$, the values of the objective function are: $J(g_0) = 3.49524$, $J(g_1) = 1.45725$, $J(g_2) = 1.45704$, $J(g_3) = 1.45626$. The initial, intermediate and optimal domains using different descent directions are presented in Figure 4 and 5. The final value of the objective function in the case *iii*) (1.45626) is less than in the case *i*)

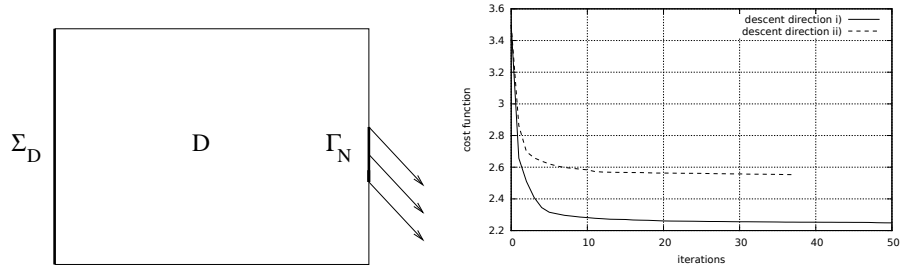


Figure 3: Cantilever. Left: Geometrical configuration of D . Right: Convergence history of the objective functions for descent directions i) given by (2.30) and ii) given by (2.31).

(2.24849) which is less than in the case ii) (2.55336). We also observe that the volume of final domain in the case iii) is larger than in the case i) or ii). These results are influenced by $\ell = 0.5$ which means that the material is “cheap”. In the case where ℓ is large, in other words, the material is “expensive”, the final domains will have smaller volumes. The acting forces are the same and smaller volumes allow larger displacements and larger compliances.

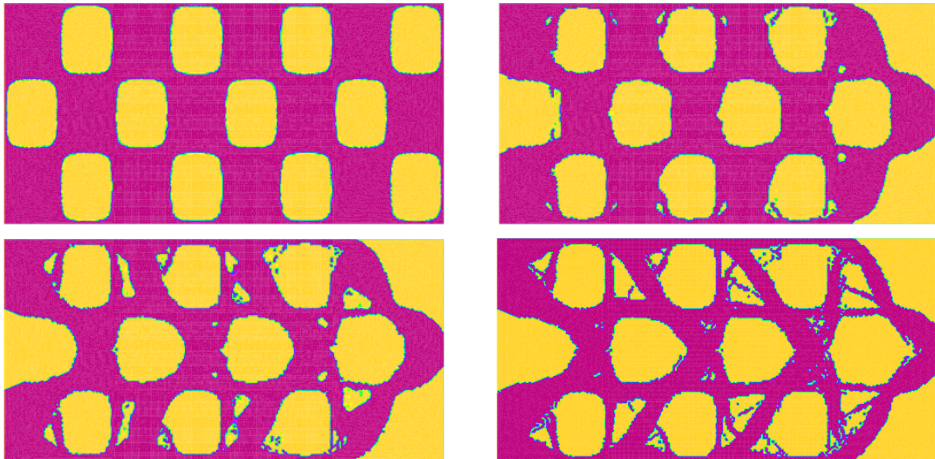


Figure 4: Cantilever. Initial (top, left), intermediate and optimal (bottom, right, after 50 iterations) domains using descent direction i).

We have tested the dependence on ϵ of the optimal solution given by the algorithm presented in this paper. We use the same mesh, the same initial domain given by $g_0(x_1, x_2) = 0.1 - \sin(4\pi x_1) \sin(3\pi(x_2 - 0.5))$ and the descent direction i) given by (2.30).

For small ϵ , the value of $c(\epsilon)$ from Proposition 2.1 is close to zero, then solving

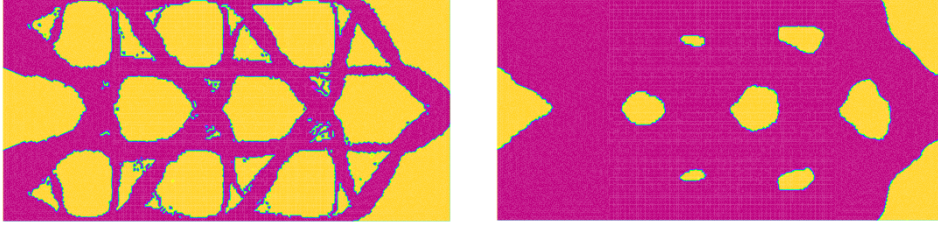


Figure 5: Cantilever. Optimal domains using descent directions *ii*) given by (2.31) (left, after 38 iterations) and *iii*) given by (2.32) (right, after 3 iterations) for the initial domain as in Figure 4.

numerically the linear system associated to (2.10) is difficult. We have replaced in (2.10), H^ϵ by

$$\widehat{H}^\epsilon(r) = \begin{cases} 1 - \frac{1}{2}e^{-\frac{r}{\epsilon}}, & r \geq 0, \\ \max(0.0001, \frac{1}{2}e^{\frac{r}{\epsilon}}), & r < 0. \end{cases}$$

For $\epsilon = 10^{-3}$, the initial objective function is 3.52187. The stopping test **Step 3** is obtained for $n = 38$, the final objective function is 2.29428 and we denote the final displacement by $\mathbf{y}^{0.001}$. For $\epsilon = 10^{-4}$, the initial objective function is 3.54231, the stopping test **Step 3** is obtained for $n = 28$, the final objective function is 2.37167. Similarly, we denote by $\mathbf{y}^{0.0001}$ the final displacement. The final domains are similar to the case $\epsilon = 10^{-2}$, Figure 4, (bottom, right). The final displacement is denoted by $\mathbf{y}^{0.01}$ when $\epsilon = 10^{-2}$. We have computed the differences of the final displacements in norms L^2 and H^1 :

$$\begin{aligned} \|\mathbf{y}^{0.01} - \mathbf{y}^{0.0001}\|_{L^2(\Omega_{28})} &= 0.083864, \quad \|\mathbf{y}^{0.01} - \mathbf{y}^{0.0001}\|_{H^1(\Omega_{28})} = 0.382696, \\ \|\mathbf{y}^{0.001} - \mathbf{y}^{0.0001}\|_{L^2(\Omega_{28})} &= 0.066597, \quad \|\mathbf{y}^{0.001} - \mathbf{y}^{0.0001}\|_{H^1(\Omega_{28})} = 0.362007. \end{aligned}$$

Example 2. Bridge

We have $D =]-1, 1[\times]0, 1.2[$, $\Sigma_D = (]-1, -0.9[\cup]0.9, 1[) \times \{0\}$, $\Gamma_N =]-0.1, 0.1[\times \{0\}$, see Figure 6 left. We work with Young modulus $E = 1$, Poisson ratio $\nu = 0.3$ and $\rho = 0.6$. The volume load is $\mathbf{f} = (0, 0)$, the surface load on Γ_N is $\mathbf{h} = (0, -1)$ and the parameter in the objective function associated to the volume of the structure is $\ell = 0.1$.

We use for D a mesh of 54510 triangles and 27576 vertices. We set $\epsilon = 10^{-2}$ for the penalization parameter and $tol = 10^{-6}$, $N = 100$ for the stopping tests.

The initial domain is obtained for

$$g_0(x_1, x_2) = 0.1 - \sin(4\pi(x_1 - 0.125)) \sin(4\pi(x_2 - 0.5))$$

and the initial value of the objective function is $J(g_0) = 0.574918$. The algorithm stops after 100 iterations (**Step 5**) when using descent directions *i*) and after 80 iterations

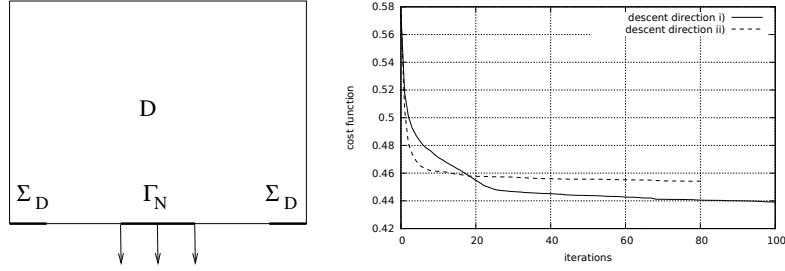


Figure 6: Bridge. Left: Geometrical configuration of D . Right: Convergence history of the objective functions for descent directions $i)$ and $ii)$.

(**Step 6**) when using descent directions $ii)$, the optimal value of the objective function is 0.43918 in the case $i)$ and 0.454161 in the case $ii)$. The initial, intermediate and the optimal domains using different descent directions are presented in Figure 7 and 8. The descent direction $iii)$ did not work properly in this example.

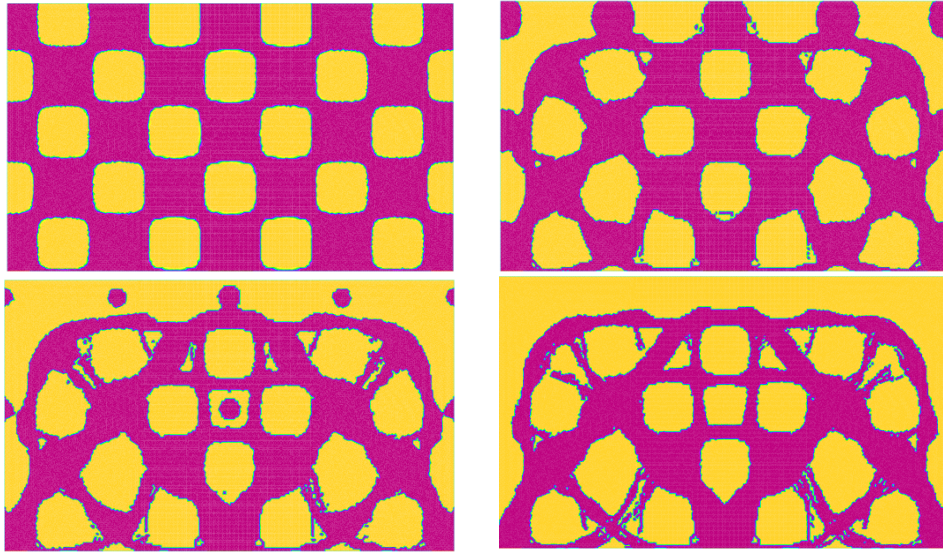


Figure 7: Bridge. Initial (top, left), intermediate and optimal (bottom, right, after 100 iterations) domains using descent direction $i)$.

Furthermore, we have used for the initialization $\Omega_0 =] - 1, 1[\times] 0, 0.6[$ obtained for $g_0(x_1, x_2) = 0.1(0.6 - x_2)$. The initial value of the objective function is $J(g_0) = 0.353644$ and the value after 100 iterations (**Step 5**) is $J(g_{100}) = 0.296596$. The optimal domain is presented in Figure 9. We have also solved the original elasticity problem (1.1)-(1.4), for the initial and final domains. Using **FreeFem++**, it is possible to build a mesh

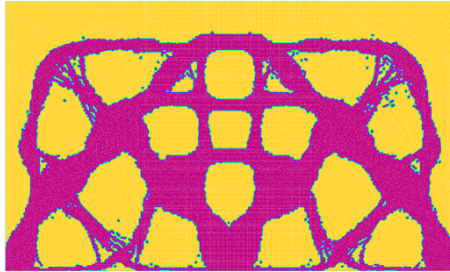


Figure 8: Bridge. Optimal domain using descent directions $ii)$ after 80 iterations, for the initial domain as in Figure 7.

which boundary is the zero level set of a function g . From Proposition 2.2, the solution computed in a mesh of Ω_g is close to the solution of (2.10) computed in a fixed mesh of D . The deformations are presented in Figure 10. The values of the cost (1.7) are 0.378632 for the initial domain and 0.297857 for the final domain.

The above final domains, that are not necessarily globally optimal, differ from the solutions obtained using homogenization or level set methods, [3], [2]. This is no contradiction since the considered optimization problems are highly non convex and the solutions depend on the initial iteration, or on the chosen parameters, etc. The important characteristic is that the method discussed in this paper ensures a consistent decrease of the cost together with topological and boundary variations for the obtained domains.

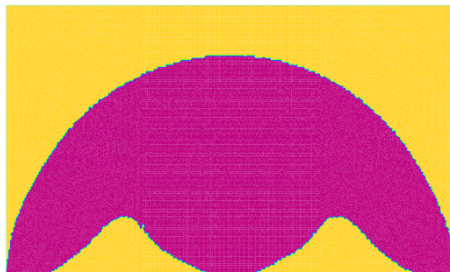


Figure 9: Bridge. Optimal domain using descent directions $i)$ after 100 iterations, for the initial domain $\Omega_0 =] - 1, 1[\times] 0, 0.6[$, the bottom half of D .

Finally, we have also tested the dependence on ϵ of the state solution of (2.10) and Prop. 2.2 was confirmed. The errors in the norms L^2 and H^1 are reported in Table 1 for the initial domain $\Omega_0 =] - 1, 1[\times] 0, 0.6[$ and in Table 2 for the final domain Ω_{100} . The reference displacement \mathbf{y}^* is the solution of (2.10) with \widehat{H} in place of H^ϵ , where $\widehat{H}(r)$ takes 1 for $r \geq 0$ and it takes 10^{-9} for $r < 0$.

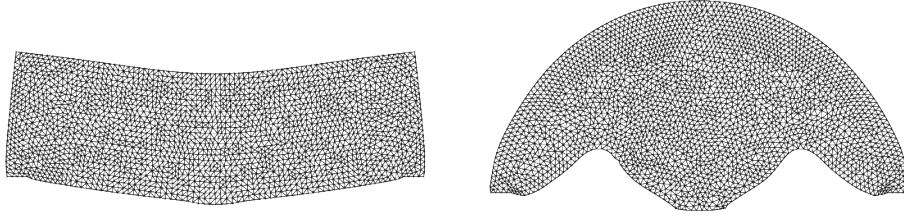


Figure 10: Bridge. The meshes after the elastic deformations for the initial domain $\Omega_0 =]-1, 1[\times]0, 0.6[$ and for the optimal domain Ω_{100} presented in Figure 9. The displacements were reduced by a factor 0.1. The cost (1.7) decreases from 0.378632 (left image) to 0.297857 (right image).

| ϵ | J | $\ \mathbf{y}^\epsilon(g_0) - \mathbf{y}^*\ _{L^2(\Omega_0)}$ | $\ \mathbf{y}^\epsilon(g_0) - \mathbf{y}^*\ _{H^1(\Omega_0)}$ |
|------------|----------|---|---|
| 0.01 | 0.353644 | 0.097841 | 0.302369 |
| 0.005 | 0.369480 | 0.035030 | 0.112965 |
| 0.001 | 0.378150 | 0.002096 | 0.027376 |
| 0.0005 | 0.378506 | 0.000799 | 0.026536 |

Table 1: The dependence of the cost given by (1.7) and of the displacement $\mathbf{y}^\epsilon(g_0)$ solution of (2.10) in the initial domain $\Omega_0 =]-1, 1[\times]0, 0.6[$. The cost for \mathbf{y}^* is 0.378727.

| ϵ | J | $\ \mathbf{y}^\epsilon(g_{100}) - \mathbf{y}^*\ _{L^2(\Omega_{100})}$ | $\ \mathbf{y}^\epsilon(g_{100}) - \mathbf{y}^*\ _{H^1(\Omega_{100})}$ |
|------------|----------|---|---|
| 0.01 | 0.296596 | 0.018279 | 0.105998 |
| 0.005 | 0.297032 | 0.005071 | 0.084750 |
| 0.002 | 0.297813 | 0.002263 | 0.076559 |
| 0.001 | 0.298063 | 0.001925 | 0.073167 |

Table 2: The dependence of the cost given by (1.7) and of the displacement $\mathbf{y}^\epsilon(g_{100})$ solution of (2.10) in the final domain Ω_{100} . The cost for \mathbf{y}^* is 0.298536.

The differences between \mathbf{y}^* and the original elasticity problem (1.1)-(1.4) are 0.000362 and 0.057692 in the norms L^2 and H^1 respectively for the initial domain Ω_0 . The cost difference is $|0.378727 - 0.378632| = 0.000095$. For the final domain Ω_{100} , the differences are 0.002925 and 0.110506 in the norms L^2 and H^1 respectively and the cost difference is $|0.298536 - 0.297857| = 0.000679$. We notice that the descent property remains valid in the original shape optimization problem as well, due to the good approximation provided by our fixed domain approach.

References

- [1] G. Allaire, *Conception optimale de structures*, Springer, 2007.
- [2] G. Allaire, C. Dapogny and P. Frey, Shape optimization with a level set based mesh evolution method, *Comput. Methods Appl. Mech. Engrg.* **282** (2014), 22–53.
- [3] G. Allaire, F. Jouve and A.-M. Toader, Structural optimization using sensitivity analysis and a level-set method, *J. Comput. Phys.* **194** (2004), no. 1, 363–393.
- [4] G. Allaire, <https://portail.polytechnique.edu/cmap/fr/boite-outils-freefem-pour-loptimisation-de-formes>, the files `levelset-cantilever.edp` and `pont.homog.struct.edp`
- [5] M.P. Bendsoe, *Optimization of structural topology, shape, and material*, Springer-Verlag, Berlin, 1995.
- [6] M.P. Bendsoe and O. Sigmund, *Topology optimization. Theory, methods and applications*, Springer-Verlag, Berlin, 2003.
- [7] M. Burger, A framework for the construction of level set methods for shape optimization and reconstruction, *Interfaces Free Bound.* **5** (2003), no. 3, 301–329.
- [8] P.G. Ciarlet, *Mathematical elasticity. Vol. I. Three-dimensional elasticity*, Studies in Mathematics and its Applications, 20. North-Holland Publishing Co., Amsterdam, 1988.

- [9] G. Delgado, *Optimization of composite structures: A shape and topology sensitivity analysis*, PhD, École Polytechnique, 2017.
- [10] J.E. Dennis Jr. and R.B. Schnabel, *Numerical methods for unconstrained optimization and nonlinear equations*, Classics in Applied Mathematics, 16. Society for Industrial and Applied Mathematics, Philadelphia, PA, 1996.
- [11] A. Halanay, C.M. Murea and D. Tiba, Existence of a steady flow of Stokes fluid past a linear elastic structure using fictitious domain, *J. Math. Fluid Mech.*, **18** (2016), no. 2, 397–413.
- [12] F. Hecht, New development in FreeFem++, *J. Numer. Math.*, **20** (2012) 251–265. <http://www.freefem.org>
- [13] H. Kawarada and M. Natori, An application of the integrated penalty method to free boundary problems of Laplace equation, *Numer. Funct. Anal. Optim.* **3** (1981) 1–17.
- [14] R.A.E. Makinen, P. Neittaanmaki and D. Tiba, On a fixed domain approach for a shape optimization problem, in *Computational and applied mathematics, II (Dublin, 1991)*, North-Holland, Amsterdam, (1992), 317–326.
- [15] P. Neittaanmaki, A. Pennanen and D. Tiba, Fixed domain approaches in shape optimization problems with Dirichlet boundary conditions, *Inverse Problems*, **25** (2009) 1–18.
- [16] P. Neittaanmaki and D. Tiba, Fixed domain approaches in shape optimization problems, *Inverse Problems*, **28** (2012) 1–35.
- [17] P. Philip and D. Tiba A penalization and regularization technique in shape optimization problems, *Siam J. Control Optim.* **51** (2013) 4295–4317.
- [18] P.-A. Raviart and J.-M. Thomas, *Introduction à l'analyse numérique des équations aux dérivées partielles*. Dunod, 2004.
- [19] D. Tiba and C.M. Murea, Optimization of a plate with holes, *Comput. Math. Appl.*, **77** (2019) 11, 3010–3020.
- [20] D. Tiba, A penalization approach in shape optimization, *Atti Accad. Pelorit. Pericol. Cl. Sci. Fis. Mat. Nat.*, **96**, No. 1, A8 (2018) [10 pages] DOI: 10.1478/AAPP.961A8